



OPEN

New Insights into the Mechanisms of Gene Electrotransfer – Experimental and Theoretical Analysis

SUBJECT AREAS:
TRANSFECTION
PERMEATION AND TRANSPORT

Mojca Pavlin & Maša Kandušer

Received
13 October 2014Accepted
11 February 2015Published
16 March 2015

Correspondence and requests for materials should be addressed to M.P. (mojca.pavlin@fe.uni-lj.si) or M.K. (masa.kanduser@fe.uni-lj.si)

Faculty of Electrical Engineering, University of Ljubljana, Tržaška 25, 1000 Ljubljana, Slovenia.

Gene electrotransfer is a promising non-viral method of gene delivery. In our *in vitro* study we addressed open questions about this multistep process: how electropermeabilization is related to electrotransfer efficiency; the role of DNA electrophoresis for contact and transfer across the membrane; visualization and theoretical analysis of DNA-membrane interaction and its relation to final transfection efficiency; and the differences between plated and suspended cells. Combinations of high-voltage and low-voltage pulses were used. We obtained that electrophoresis is required for the insertion of DNA into the permeabilized membrane. The inserted DNA is slowly transferred into the cytosol, and nuclear entry is a limiting factor for optimal transfection. The quantification and theoretical analysis of the crucial parameters reveals that DNA-membrane interaction (N_{DNA}) increases with higher DNA concentration or with the addition of electrophoretic LV pulses while transfection efficiency reaches saturation. We explain the differences between the transfection of cell suspensions and plated cells due to the more homogeneous size, shape and movement of suspended cells. Our results suggest that DNA is either translocated through the stable electropores or enters by electro-stimulated endocytosis, possibly dependent on pulse parameters. Understanding of the mechanisms enables the selection of optimal electric protocols for specific applications.

One of the promising methods for delivery of genetic material into a cell is gene electrotransfer, which uses locally delivered electric pulses (electroporation) to transfer DNA into the cell^{1,2}. The first *in vivo* gene electrotransfer was demonstrated in the early nineties of the last century by Titomirov³ and by several other independent studies^{4–8} and has since then been extensively studied^{9–12}. In contrast to viral vector transfer, the use of electric pulses for gene delivery represents a safer method, which is not hampered by concerns of immunogenicity and pathogenicity¹³. Different protocols were designed for *in vitro* and *in vivo* applications, either employing short hundreds-of-microsecond pulses⁴, long millisecond pulses^{7,8,14} or combining high-voltage (10–1000 μ s) and low-voltage (10–400 ms) pulses^{12,15–19}. We have recently shown *in vitro* that^{20,21} longer electric pulses are optimal for high transfection efficiency but reduce viability, while shorter pulses enable moderate transfection efficiency and preserve viability. For clinical applications it is also crucial to achieve sufficient transfection efficiency in a given target tissue (e.g. tumor, muscle, skin)^{10,22}. Gene electrotransfer has in recent years emerged as the most promising non-viral method for delivery of plasmid DNA (pDNA), oligonucleotides and short RNA molecules in gene therapy for a series of conditions like cancer, autoimmune and inflammatory diseases²³. The first successful clinical trials have already been completed¹¹. Recently it has been identified as an ideal method for DNA vaccination for hepatitis, HIV and cancer treatment^{24–26} since electric pulses play a dual role; they enable gene delivery and act as an adjuvant.

However, several papers stress that the mechanisms of gene electrotransfer are still not fully understood^{10,23,27,28}. The current description of the process defines several steps: i) electropermeabilization of the cell membrane, ii) contact of the pDNA with the cell membrane (formation of a complex), iii) translocation across the membrane, iv) transfer to and into the nucleus and gene expression^{10,18,19,29,30}. In addition, new observations of the role of the cytoskeleton and endocytosis have also been published^{31,32}. From the perspective of clinical applications, all of these steps relate to the barriers which must be overcome for sufficient DNA delivery and expression in the target tissue.

- i) The first step is cell membrane electropermeabilization, where electric pulses are applied and the transmembrane voltage is induced due to Maxwell-Wagner polarizations. Above a critical (threshold) trans-



membrane potential (between 0.2–1 V), a high electric field leads to the formation of hydrophilic pores, thus enabling the transfer of molecules into cells². Ions and small molecules enter the cells by free diffusion through pores during and after pulse delivery^{33,34}, while the transfer of large pDNA is not governed by diffusion, but is a more complex process^{15,18,19,29,30,34}.

- ii) The second step is the interaction of the DNA with the permeabilized cell membrane. It was shown that DNA has to be present in close proximity of the cell membrane at the moment of pulse delivery, enabling contact between the DNA and the electropermeabilized membrane^{16,17,20,21,29,30,35,36}. The DNA-membrane complex formation was first suggested when the effect of divalent cations^{37–39} on electrotransfection was studied. The complex presents binding to the membrane or partial insertion of DNA in the permeabilized cell membrane^{15,16,19,29,30}. The first visualization performed by labeling DNA with fluorescent dye TOTO-1⁴¹ showed complex formation only on the cathodic side of the cell. In addition, within tissues the extracellular matrix represents another barrier which reduces the amount of DNA interacting with the target cells, by hindering the homogeneous distribution of the injected DNA and by decreased DNA mobility during electric pulses^{40–42}. The free diffusion of DNA is almost negligible compared to electrophoretic drag, therefore, the selection of sufficiently high and long pulses is important^{12,16,17,21,40,43}.
- iii) The third step is the transfer of DNA into the cells. The process of DNA transfer across the cell membrane has not been directly visualized yet. The DNA enters the cytoplasm several minutes after pulse application^{41,48}; first the contact of the DNA with the permeabilized cell membrane is formed^{15,19,34,44}, then the DNA is either translocated across the cell membrane by an unidentified mechanism^{20,23}, or alternatively, the DNA enters the cells by electric-field-stimulated endocytosis^{32,45,46}. Recently³², it was suggested that endocytosis could play an important role in gene electrotransfer, however, our results do not support this hypothesis⁴⁷.
- iv) The last step for efficient electrotransfer is the intracellular trafficking of the DNA through cytosol and nuclear import. Different cytoplasmic structures hinder DNA mobility inside the cytosol, and foreign DNA is also exposed to DNase activity^{48,49}. It was demonstrated that⁵⁰ pDNA is probably actively transferred to the nucleus via the tubulin network. Further, during mitosis when the nuclear envelope is disintegrated, the highest electrotransfer efficiency was obtained⁵¹. It was shown that plasmids containing a nuclear-localization-sequence (NLS) that enables active transport across nuclear pores increased the gene electrotransfer efficiency^{50,52,53}.

In spite of numerous experimental studies, only a few are combined with a theoretical description of DNA-membrane interaction^{34,37}, the quantification of the number of plasmid DNA⁵⁴ or the DNA mobility in a complex environment such as tissue^{40,41,55}. In this paper we present a systematic *in vitro* analysis of all the steps of gene electrotransfer. In addition, the differences between cells in a suspension and plated cells are discussed. The most undefined process is the mode of DNA transfer across the cell membrane. We approached this question by different pulse combinations of high-voltage (HV) and low-voltage (LV) pulses (e.g. HV+LV, LV+HV), enabling separate analysis of electropermeabilization and electroporation. Our results provide new insights into the processes important for further development of *in vitro* gene electrotransfer protocols for biotechnological and biomedical applications.

Methods

Cell cultures, electropermeabilization buffers and plasmid. Chinese hamster ovary CHO cells (European Collection of Cell Cultures) were grown in F12 HAM (Gibco)

supplemented with 1 mM L glutamine, 10% fetal bovine serum (PAA, Austria) and antibiotics at 5% CO₂ and 37°C. Most of the experiments were performed on cells in the early exponential growth phase (24 h after trypsinization). To evaluate the effect of the stage of the cell culture, cells in the early plateau phase (72 h after trypsinization) arrested in the G1 stage of the cell cycle were used. The electropermeabilization buffer was iso-osmolar 10 mM NaH₂PO₄/Na₂HPO₄, 1 mM MgCl₂ and 250 mM sucrose, pH = 7.2, while for the visualization of the DNA-membrane interaction with TOTO, we used 10 mM KH₂PO₄/K₂HPO₄ with the same additives. For all gene electrotransfer experiments, we used plasmid pEGFP-N1 (Clontech Laboratories Inc., Mountain View, CA, USA).

Electric pulse protocols. Three different pulsing protocols, consisting of either high-voltage HV pulses only, low-voltage LV pulses only, or a combination of both HV and LV pulses (HV-LV combinations) were used for both plated cells and cells in suspensions. To generate electric pulses, a CliniporatorTM (Igea, Italy) and a prototype of the electric pulse generator described in Ref. 19 were used. Parallel wire electrodes were used for the plated cells¹⁸ and parallel plate electrodes (Eppendorf, Germany) for cell suspension. The distance between the electrodes was 4 mm. All the experiments were repeated at least three times at different dates. In all experiments, the standard HV pulses were 4 × 200 μs pulses, 1 Hz with pulse amplitude $U = 400$ V (applied electric field $E_{HV} = 1$ kV/cm), except in experiments where E was varied, and the standard LV pulse was 1 × 100 ms, with pulse amplitude 30 V ($E_{LV} = 0.075$ kV/cm – LV_{30}), except in experiments where higher LV was also used $E_{LV} = 0.137$ kV/cm (LV_{55}). In the HV+LV protocol, the LV pulse was applied after the HV, with a lag of 20 ms^{18,19}, while for the LV+HV protocol, the sequence was reversed.

Cell membrane permeabilization. Cell membrane permeabilization was determined by the uptake of 150 μM propidium iodide (PI) (Invitrogen, Germany), added immediately before electropermeabilization. For each experiment, a negative control - cells not exposed to an electric field, and positive control - cells exposed to 1.8 kV/cm (100% permeabilization) were prepared. The fluorescence intensity was determined 3 minutes after electropermeabilization in a microplate reader (Tecan, Austria) at a 535/617 nm (excitation/emission) wavelength. The percentage of electropermeabilized cells was calculated as the relative fluorescence intensity vs. the positive control³⁶.

Viability. For plated cells, viability was determined by a manual cell count under bright field optics on an inverted microscope (Zeiss 200, Axiovert, Germany) at 20× objective magnification. The cell viability was calculated as the ratio between the number of all cells counted in the treated sample and the number of all cells in the control sample^{18,47}. For cell suspensions, viability was determined by clonogenic assay. After electropermeabilization, cells were plated in concentrations of 250 cells per 60 mm Petri dish and grown for six days. The colonies were counted and the viability (%) was determined as the ratio between the number of colonies in the treated sample and the number of all cells in the control sample that were not exposed to electric pulses.

Electrotransfer of plasmid DNA. Plated cells: 5 × 10⁴ cells were seeded in 24 multiwell plates and maintained in culture for 24 h, then the growth media was replaced with a pulsing buffer containing different concentrations of the plasmid DNA (c_{DNA}). After a 2–3 min incubation, samples were electropermeabilized, fetal bovine serum (PAA, Austria) was added (37 μl) and the cells were grown for another 24 h in the culture medium. The next day, the electrotransfer efficiency was determined by fluorescent microscopy (Zeiss 200, Axiovert, Germany, at 488/509 nm). At least 7 images were acquired per parameter for each experiment and the percentage transfection (%TR) was determined as a ratio between the fluorescent cells and the total number of cells counted under bright field optics¹⁸. For HV-LV pulsing protocols, the average maximal fluorescence intensity – FL^{GFP} [A.U.] was also determined.

Cells in suspension: cell cultures were trypsinized 24 hours before the experiments. On the day of experiment, a cell suspension of 2.5 × 10⁶ cells/ml was prepared in an electropermeabilization buffer. The optimal c_{DNA} was 40 μg/ml, while sub-optimal c_{DNA} were 10 μg/ml and 5 μg/ml. In addition, we also tested $c_{DNA} = 100$ μg/ml. The electropermeabilization procedure was the same as for plated cells. Cells were plated in 25 cm² culture dishes for 24 hours. The next day, we prepared a cell suspension (1 × 10⁶ cells/ml) in phosphate-buffered saline (PBS) and the GFP expression was measured by flow cytometry with a Coulter EPICS Ultra flow cytometer (Beckman Coulter Electronics) and with a CyFlow space flow cytometer (Partec). For each sample, 10000 cells were analyzed. The collected data were analyzed using FlowJo (Tree Star) software. From this percentage of transfected cells and average fluorescence intensity were obtained.

Visualization of DNA-membrane interaction and plasmid localization in the cytosol. To visualize DNA interaction with the cell membrane, we stained pEGFP-N1 with 2.3 × 10⁻⁴ M TOTO-1 nucleic acid stain (Molecular Probes – Invitrogen, Carlsbad, California, USA) as described in Ref. 29. Cells (1 × 10⁵ cells/ml) were plated in a Labtech chamber for 1 h in a cell culture medium. Then electropermeabilization media with TOTO-labeled DNA (10 μg/μl and $c_{DNA} = 2$ μg/μl to obtain a detectable fluorescence) was added to the cells and different combinations of HV and LV pulses were applied. The HV amplitude was 1.4 kV/cm. The interaction of the DNA with the membrane was determined by fluorescent microscopy (Zeiss 200, Axiovert, Germany) at 100× objective magnification at 514/533 nm. The TOTO fluorescence intensity (FL^{TOTO}) profiles were analyzed (MetaMorph) and the average maximal fluorescence intensity – FL^{TOTO} [A.U.] was obtained from recorded images (at least 5

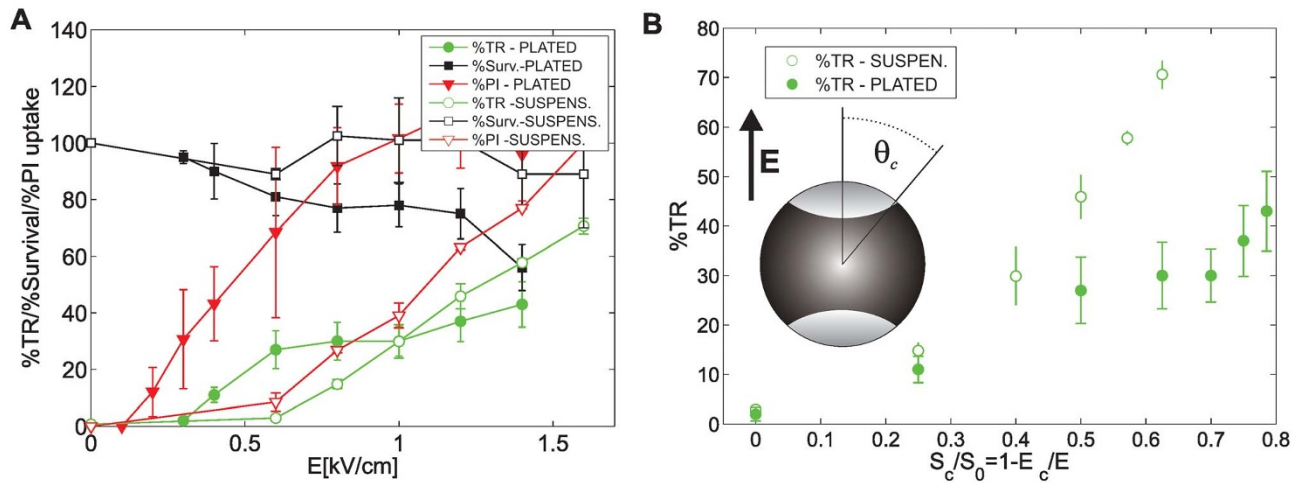


Figure 1 | (A) Effect of electric field strength on the percentage transfection of CHO cells (%TR), viability (%Survival) and electroporation (%PI uptake) for $4 \times 200 \mu\text{s}$ pulses (HV) and 1 Hz repetition frequency. Results are shown for plated cells (closed symbols) and cells in a suspension (open symbols) and are presented as mean \pm standard error of at least three independent experiments. (B) Dependence of %TR on the fraction of permeabilized membrane area S_c/S_0 as given in Eq. 3, for plated cells and cells in a suspension. The bright shaded surface of the spherical cell represents the permeabilized cell membrane - S_c .

images per parameter for each experiment). For localization of the plasmid in the cytosol, the plasmid was labeled with rhodamin dye (TM-Rhodamin, Mirus, USA), observed at $100\times$ objective magnification.

Stage of the cell culture. Gene electrotransfer was performed in cell suspensions trypsinized 24 h before the experiment, or on cells cultured for 72 h, to obtain confluent cell cultures in the early plato phase arrested in the G1 phase of the cell cycle. Three independent experiments were performed.

Analytical calculations. Calculation of the permeabilized surface of the cell membrane. If a cell is exposed to an external electric field E , a transmembrane voltage U_m is induced on the cell membrane. When U_m exceeds the threshold voltage U_c , then the part of the cell membrane where $|U_m| > U_c$ is permeabilized². For a spherical cell of radius R , a well-known form of U_m for physiological conditions^{34,56} is valid:

$$U_m = 1.5 ER \cos \theta, \quad (1)$$

where θ is the angle that defines the point on the membrane with respect to the field direction. The above equation is valid for spherical cells, while for spheroidal cells a similar equation is valid taking into account also the shape of the cells⁵⁷. One can define the critical angle θ_c , as the angle where the transmembrane voltage equals the critical voltage:

$$U_c = 1.5 ER \cos \theta_c, \quad (2)$$

while the critical electric field E_c is defined as E where $\theta_c = 0$, therefore: $E_c = U_c/1.5R$. From this, the total area exposed to an above-threshold transmembrane voltage - the permeabilized area - can be obtained:

$$S_c = S_0(1 - E_c/E), \quad (3)$$

where S_0 is total surface of the cell membrane.

Analysis of DNA electrophoresis during HV and LV pulses. Electrophoresis is one of the mechanisms that was shown to be important for the efficient delivery of DNA molecules into cells by electric pulses^{15,16}, especially when plasmid concentration is relatively low^{18,19}. We present the calculation of the average traveled distance - L of a pDNA in aqueous solutions, and from this we estimate the number of DNA molecules available for contact with the permeabilized cell membrane (N_{DNA}) for our in vitro conditions. We have followed the derivation of Zaharoff and Yuan⁴¹. Briefly, the electrophoretic force acts on the negatively charged DNA molecules and drags it toward the cathodic side of the cell membrane: $F = e_{eff} E$, where the effective charge (e_{eff}) depends on the ionic strength of the solution and the length of the plasmid ($e_{eff} = 0.066 e$ per base pair $\times 4.7$ kbp for pEGFP plasmid). We can use the approximation that during the electric pulses we have a steady-state condition⁴¹, thus:

$$v = \mu E, \quad \mu = e_{eff}/f = \frac{e_{eff}}{6\pi\eta R_g}, \quad (4)$$

where v is velocity of the molecular movement, μ is electrophoretic mobility and f is the Stokes' frictional drag, $R_g \approx 100$ nm is the approximate radius of gyration and $\eta = 0.01 \text{ g cm}^{-1} \text{ s}^{-1}$ is the viscosity of the medium. In all calculations, E represents the homogeneous electric field strength, which is justified for our geometry of two parallel electrodes. The distance L traveled due to electrophoresis can be thus calculated from

the total duration of the electric pulses t_E :

$$L = v t_E = \mu E t_E. \quad (5)$$

Here we have to stress that the mobility μ of a DNA molecule during electric pulses is a complex function of the electric field strength, due to several effects like the elongation and orientation of DNA molecules in the electric field. Therefore, mobility is not the same for HV or LV pulses, however, as already shown⁴¹, we can use the approximation of constant μ for our conditions. For a 4.7 kbp supercoiled pEGFP, μ is similar as in Ref. 34: $\mu = 1.5 \times 10^4 \mu\text{m}^2/\text{Vs}$; where 4.3 kbp pDNA was used, a similar value can be obtained directly from Eq. 4.

Results

Electroporation, electrotransfection and cell viability for different electric field strengths. In Fig. 1A, we present the effect of the electric field strength (E) on the electroporation (%PI positive cells), percentage transfection (%TR) and survival (%viable cells) for a train of four high-voltage pulses (HV) of $200 \mu\text{s}$ duration and 1 Hz repetition frequency for plated cells and for cells in a suspension. Electroporation increased above a certain electric field threshold (E_c) and electrotransfer occurred only above the E_c . In a suspension, much higher maximal %TR was achieved (70%) compared to plated cells (40%), even though in both cases the maximal electroporation was reached (around 100%). Plated cells were more affected by electric pulses in terms of cell survival, namely viability dropped to 55%, while for cells in suspension it was maintained at approximately 90% at the highest electric fields (>1.4 kV/cm). In Fig. 1B, the %TR is presented with respect to the electroporated membrane area (Eq. 3).

Role of electrophoresis - effect of plasmid concentration on electrotransfer efficiency. We studied electroporation of the cell membrane, electrophoresis and DNA-membrane interaction by applying combinations of HV and LV pulses (HV, LV, HV+LV, LV+HV).

Electroporation for different HV and LV pulses. In order to separate the electrophoretic effect of LV pulses from electroporation, we determined the PI uptake for different combinations of HV and LV pulses on plated cells and two different pulse amplitudes for LV pulses (30 V and 55 V). We obtained a nearly 100% electroporation for the HV, HV+LV₃₀ and HV+LV₅₅ pulsing protocols. No statistically significant PI uptake was obtained with the LV₃₀ pulse, while for the LV₅₅ pulse, PI uptake was 5%. A higher percentage transfection (%TR) was observed for both combinations



of HV+LV protocols (HV+LV₃₃ and HV+LV₅₅) and approximately 2% of cells were transfected with only the LV₅₅ pulse (results not shown). Therefore, only electrophoretic non-permeabilizing LV₃₀ pulses were used in further experiments with LV pulse.

The effect of plasmid concentrations on the electrotransfection efficiency for different HV and LV pulses – the role of electrophoresis. In Fig. 2 the effect of HV and LV pulses on the gene electrotransfer efficiency (%TR and fluorescence intensity of FL^{GFP}) for different c_{DNA} for cells in suspension and plated cells are presented. For cells in suspension (Figs. 1 B and D), the %TR and mean fluorescence intensity FL^{GFP} obtained by flow cytometry are shown. We obtained that at c_{DNA} = 100 µg/ml, no increase in %TR was obtained for HV+LV pulses compared to HV only (Fig. 2B). For all lower plasmid concentrations (c_{DNA} = 40, 10 and 5 µg/ml), an increase was obtained for HV+LV compared to HV pulses (statistically significant only at 5 µg/ml, P = 0.044). For LV pulses only, a negligible GFP expression was obtained. Similar relationships among the pulsing protocols were obtained when analyzing the mean fluorescence intensity FL^{GFP} (Fig. 2D). Again for all concentrations – up to 40 µg/ml, the HV+LV protocol led to a higher expression of GFP. Also at c_{DNA} = 100 µg/ml, there appears to be a different increase of FL^{GFP} for HV+LV vs. HV pulses only.

In Figs. 2A and C, the results for plated cells are shown, where the percentage transfection (%TR) and fluorescence intensity (FL^{GFP}) were determined by fluorescence microscopy. For HV pulses, the %TR was directly dependent on the plasmid concentration; at c_{DNA} = 10 µg/ml, the % TR was 25%, which dropped to only 6% at c_{DNA} = 1 µg/ml. The HV+LV at c_{DNA} = 1 µg/ml lead to a

significant increase (P < 0.001) in the percentage transfection (23%) compared to HV pulses only (6%). At 5–10 µg/ml plasmid concentrations, the LV pulse did not significantly affect the %TR (P > 0.05). It is important to note that the optimal plasmid concentration for plated cells was 10 µg/ml, while sub-optimal c_{DNA} were 5 µg/ml and 1 µg/ml.

To further investigate the role of electrophoresis on plated cells, we used an additional pulsing protocol consisting of LV pulse applied before the HV pulses (LV+HV). The LV+HV protocol at c_{DNA} = 1 µg/ml significantly increased the %TR cells compared to HV (P = 0.043), but was still less effective than the HV+LV protocol. With only the LV pulse, a negligible number of transfected cells (less than 1%) was obtained. The average maximal fluorescence intensity FL^{GFP} (Fig. 2C) was highest for HV+LV, compared to the HV (P = 0.026) and LV+HV protocols. The increase of FL^{GFP} for the LV+HV vs. the HV protocol was obtained at c_{DNA} = 1 µg/ml, but it was not statistically significant (P > 0.05), while at c_{DNA} = 10 µg/ml, all three pulsing protocols lead to a similar %TR.

Visualization of DNA-cell membrane interaction and internalization into cytosol. Direct visualization of the DNA-membrane interaction was performed by TOTO-1 labeled pDNA for different HV-LV protocols and different c_{DNA}. For all protocols, DNA interaction with the cell membrane facing the cathode was observed, since DNA is negatively charged. Fluorescent images of treated cells exposed to HV, HV+LV, LV+HV and LV pulses are shown in Fig. 3 A. The images were acquired 2–5 min after pulsation. The fluorescence intensity FL^{TOTO} corresponds to the amount of TOTO-labeled DNA interacting with the permeabilized cell

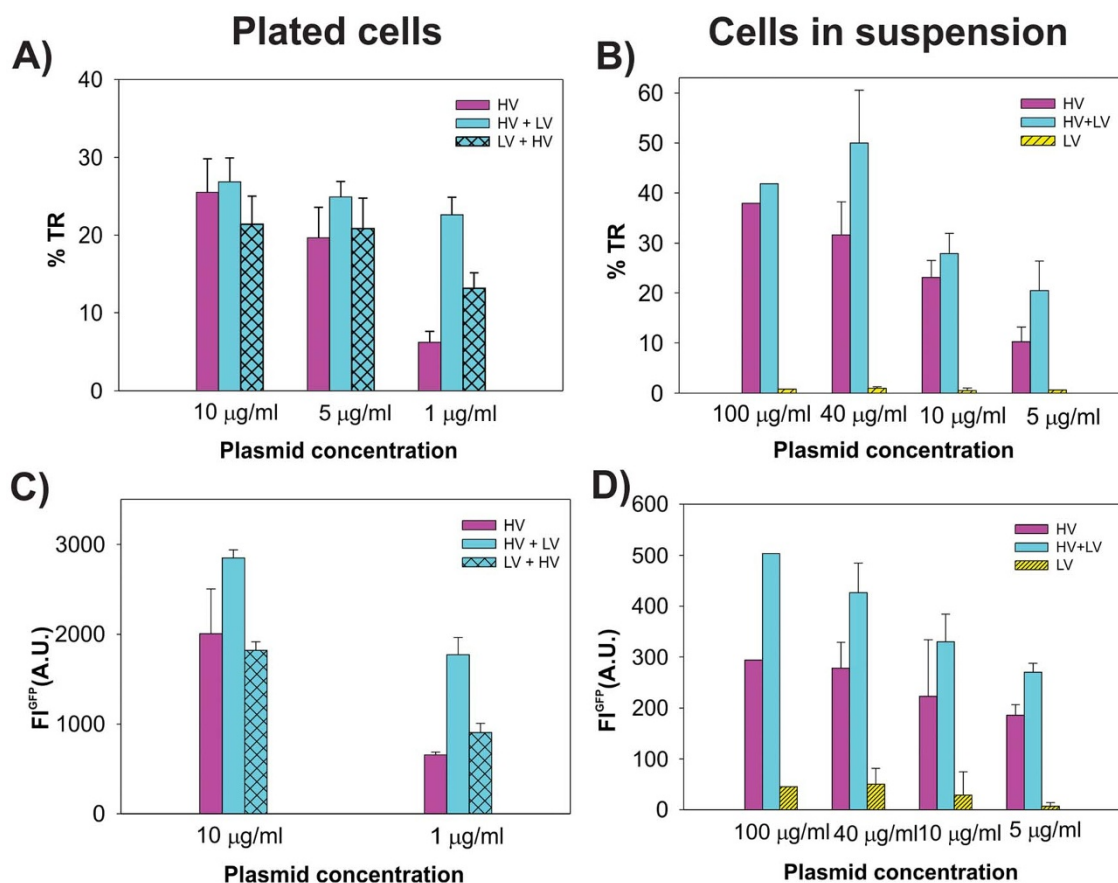


Figure 2 | Effect of different HV-LV protocols on the electrotransfer efficiency for different plasmid concentrations. Panels A and C plated cells, B and D cells in a suspension, % TR (A and B) and average maximal fluorescence intensity in A.U. Pulse parameters were: HV pulses ($4 \times 200 \mu\text{s}$), 1 Hz and $1 \times 100 \text{ ms}$ LV $E_{HV} = 1 \text{ kV/cm}$ (400 V) and $E_{LV} = 0.075 \text{ kV/cm}$. The results are presented as mean \pm standard error of at least three independent experiments.



membrane. Along the membrane, spots of high fluorescence intensity were observed for all pulsing protocols.

The values of FL^{TOTO} (A.U.) were calculated from all recorded images for each pulsing protocol. For HV+LV pulses, an approximately $3\times$ increase in FL^{TOTO} was observed compared to HV pulses only for $c_{DNA} = 10 \mu\text{g/ml}$ and an approximately $2\times$ increase of $c_{DNA} = 2 \mu\text{g/ml}$ (Fig. 3). On average, the FL^{TOTO} of LV+HV was slightly higher compared to HV pulses, but significantly smaller than for the HV+LV protocol. No interaction (the fluorescence intensity was similar to the background) was detected for the non-permeabilizing LV pulse alone. On average, more DNA interaction with the cell membrane and higher FL^{TOTO} was observed for higher amounts of TOTO-labeled DNA ($c_{DNA} = 10 \mu\text{g/ml}$) compared to sub-optimal $c_{DNA} = 1 \mu\text{g/ml}$. Further, the entry of pDNA into the cytosol was visualized by rhodamin-labeled DNA. After 10–15 minutes, labeled pDNA was observed inside the cytosol (see Discussion).

DNA entry into the nucleus. The last step and barrier for the successful electrotransfer of DNA is the nuclear import of pDNA. We designed additional experiments using cells in the exponential and plato stage of growth in order to compare the efficiency of gene electrotransfer of cells in the exponential vs. plato phase of cell culture. We obtained a significantly lower percentage transfection %TR for cells in the plato phase ($15.5\% \pm 1.1$) compared to cells in the exponential phase ($55.7\% \pm 11.6$) for both the HV and HV+LV (17.3 ± 1.4 plato vs. 52.2 ± 10.2 exponential phase) pulsing protocols as shown in Table 1. We should also stress here that our standard experimental protocol was performed on cells in the exponential phase of cell culture, which is also a standard protocol.

Theoretical analysis. In the following two subsections we: i) calculate the permeabilized surface area of the cell and ii) analyze electrophoresis for different HV-LV pulses and calculate the N_{DNA} – the number of DNA molecules available for contact with the permeabilized surface.

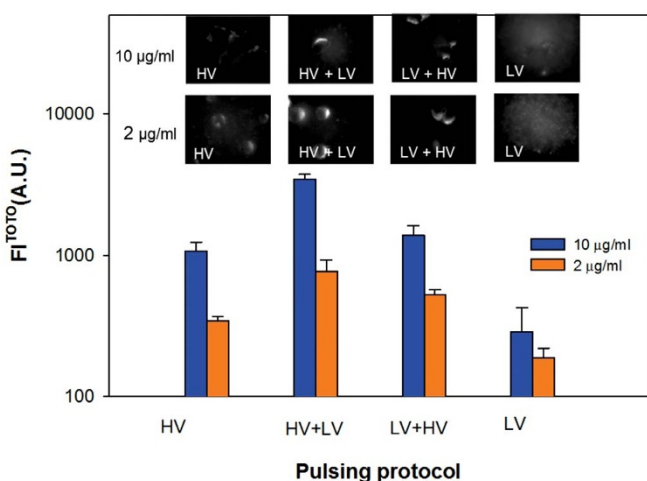


Figure 3 | DNA – membrane interaction for different HV-LV protocols for $c_{DNA} = 10 \mu\text{g/ml}$ and $2 \mu\text{g/ml}$. The average maximal fluorescence intensity FL^{TOTO} is presented as an average \pm standard error; the representative images for HV, HV+LV, LV+HV and LV pulses are shown on top. Please note that the scale of fluorescence intensity in the micrographs is adjusted between Min = 100 and Max = 700 A.U. in images with $c_{DNA} = 10 \mu\text{g/ml}$, and between Min = 100 and Max = 300 A.U. for $c_{DNA} = 2 \mu\text{g/ml}$. Immediately after the labeled plasmid was added to the cells, different combinations of HV ($4 \times 200 \mu\text{s}$, $E_{HV} = 1.4 \text{ kV/cm}$, 1 Hz) and LV pulses ($1 \times 100 \text{ ms}$, $E_{LV} = 0.137 \text{ kV/cm}$) were applied.

Calculation of the permeabilized surface of the cell membrane. The permeabilized surface S_c of the cell membrane depends on the applied field E and the threshold field E_c^{58} : $S_c = S_0(1 - E_c/E)$, where S_0 is total surface of the cell membrane. Thus E determines the area of the membrane which is permeabilized – $S_c(E)$, and consequently the electrotransfer efficiency. In Fig. 1B, dependence of the % of transfected cells on a normalized permeabilized membrane surface area S_c/S_0 (Eq. 3) is shown. For plated cells, an approximately linear dependency on the permeabilized surface was obtained, while for cells in a suspension, a non-linear increase of S_c with E was observed.

Analysis of DNA electrophoresis during HV and LV pulses and estimations of the number of DNA molecules in contact with the permeabilized cell membrane. The traveled distance (L) of pDNA during HV and LV pulses due to the electrophoretic force can be obtained from Eq. 5 (see Methods): $L = \mu E t_E$. For a single LV pulse ($1 \times 100 \text{ ms}$, 75 V/cm) we obtain $L_{LV} \approx 11 \mu\text{m}$, $L_{HV} \approx 1.2 \mu\text{m}$ and $L_{HV+LV} = 12.2 \mu\text{m}$. Thus, for HV+LV pulses the traveled distance is approximately $10\times$ longer compared to HV pulses only ($4 \times 200 \mu\text{s}$, 1 kV/cm). If we assume that the electrophoretic force drags the negatively charged DNA molecules that are at a distance less than L from a cathodic site of a cell, we can estimate the number of DNA molecules – N_{DNA} in the volume V , which are available for contact with the permeabilized part of the cell membrane. The results of the calculations of N_{DNA} for different pulsing protocols are presented in Fig. 4. Thus, if the c_{DNA} is sub-optimal, it is crucial that the DNA is electrophoretically dragged toward the membrane. For plated CHO cells we obtained the following equation for the volume V , from which the DNA molecules are dragged toward the permeabilized part of the cell membrane:

$$V_{plated} = L \pi R_{avg} h \cos^2 \theta_c = L \pi R_{avg} h (1 - (E_c^{plat}/E)^2), \quad (6)$$

where R_{avg} is average radius of the plated CHO cells³⁶ and the height of a cell is $h = 4 \mu\text{m}$. For plated cells the equation for the induced transmembrane potential for spheroidal cells is valid⁵⁷, however, since the cells are oriented randomly, the average long radius R_{avg} is a valid approximation, since cells oriented with the long axis in parallel with E are first electroporated. For cells in a suspension that are of spherical shapes, the corresponding volume is:

$$V_{suspension} = L \times \pi R^2 \cos^2 \theta_c = L \times \pi R^2 (1 - (E_c^{susp}/E)^2). \quad (7)$$

From this we can estimate the N_{DNA} available for contact formation for different c_{DNA} :

$$N_{plated} = \rho_{DNA} V_{plated}, \quad N_{suspension} = \rho_{DNA} V_{suspension}, \quad (8)$$

where ρ_{DNA} is the number density ($\rho_{DNA} = c_{DNA} N_A / M r_{DNA}$) of DNA for a given plasmid concentration. Thus, from Eqs. 6–8 we can calculate the N_{DNA} in contact with the permeabilized cell membrane as shown in Fig. 4. The N_{DNA} is directly proportional to L and consequently is approx. $10\times$ lower for HV pulses compared to HV+LV pulses (Fig. 4). From our results we can estimate that for efficient transfection in vitro, several tens of molecules have to be in contact with the cell membrane, while for a smaller $N_{DNA} < 10$ the transfection is very low (Figs. 2 and 4).

For cells in a suspension (Fig. 4B), it can be seen that in general a similar relation is obtained: approx. $10\times$ more N_{DNA} are in contact with the membrane obtained for HV+LV vs. HV pulses, which enables more DNA copies to be transferred into the cytosol, leading to a higher fluorescence intensity in agreement with experimental observations for low plasmid concentrations (Fig. 2D). Thus, the strength and length of the electric pulses determine the distance L from which the DNA can access the cell and E determines the area of the membrane which is electropermeabilized – S_c . It is also clear that since N_{DNA} linearly increases with c_{DNA} and that probability of transfection directly depends on N_{DNA} , there is a very strong correlation



Table 1 | Efficiency of gene electrotransfer in terms of % transfected cells (%TR) for CHO cells in a suspension in the exponential growth phase vs. cells in the plato phase for the HV ($4 \times 200 \mu\text{s}$, $E_{HV} = 1.4 \text{ kV/cm}$, 1 Hz) and HV+LV (HV $4 \times 200 \mu\text{s}$, $E_{HV} = 1.4 \text{ kV/cm}$, LV $1 \times 100 \text{ ms}$, $E_{LV} = 0.0375 \text{ kV/cm}$) pulsing protocols. The results are presented as mean \pm standard error of at least three independent experiments, $c_{DNA} = 40 \mu\text{g}/\mu\text{l}$

%TR PHASE OF CULTURE	HV	HV+LV	LV
exponential	55.7 ± 11.6	52.2 ± 10.2	0.3 ± 0.1
plato	15.5 ± 1.1	17.3 ± 1.4	0.1 ± 0.0

between the %TR and N_{DNA} until saturation is reached, and the %TR does not increase for higher N_{DNA} .

When comparing plated and cells in a suspension, we observed that in order to reach comparable transfection efficiencies, higher pDNA concentrations had to be used for cells in a suspension. Also, due to smaller sizes, the threshold for electrotransfer was reached at a higher E for cells in suspension compared to plated cells as shown in Ref. 36. Here we extend this study also to HV-LV pulsing combinations. Obviously, electrotransfer of plated cells behaves to some extent differently than with cells in a suspension. The saturation of the %TR for plated cells is already reached at $10 \mu\text{g}/\text{ml}$ compared to cells in suspension, where the highest %TR is reached at $40 \mu\text{g}/\text{ml}$. Also, c_{DNA} has to be higher for suspensions compared to plated cells. Moreover, in a suspension, a much higher overall maximal %TR can be obtained, both for CHO (up to 70%) and B16 cells (45%) compared to plated cells (38% for CHO and 25% for B16 cells), and also saturation is reached at a higher N_{DNA} for cells in a suspension. The results for B16 cells are presented in Ref. 36.

Calculation of electric energy. One hypothesis can be that the electric energy needed for DNA interaction with the membrane (complex formation)²⁹, is the crucial parameter for electrotransfection, since there exists an energy barrier between the negatively charged DNA and the negatively charged cell membrane. In the most simplified case, we can assume that the electric energy of the pulses W_e equals the work of the electrophoretic force $A_e = F_e \times L$. Since $L = \mu E t_E$ we obtain:

$$W_e = F_e \times L = e_{eff} \mu E^2 \times t_E, \quad (9)$$

where E is the applied electric field strength and t_E is total time

duration of all pulses. We can thus estimate W_e of our standard HV ($4 \times 200 \mu\text{s}$, 1 kV/cm), LV ($1 \times 100 \text{ ms}$, 0.075 kV/cm) and combined HV+LV pulses:

$$W_e^{LV} = k \times 0.56 s(kV/cm)^2, W_e^{HV} = k \times 0.8 s(kV/cm)^2, \quad (10)$$

$$W_e^{HV+LV} = W_e^{LV+HV} = k \times 1.36 s(kV/cm)^2.$$

where $k = e_{eff} \mu$.

The relation between electroporation, electrophoresis, DNA-membrane interaction and GFP expression. In Table 2 we summarize the main results related to the different steps (Fig. 5) of electrotransfection. Electroporation was quantified by the %PI of positive cells, DNA-membrane interaction by the analysis of the fluorescence intensity of TOTO-labeled pDNA (FL^{TOTO}), gene expression by the fluorescence intensity of GFP (FL^{GFP}) and the percentage transfection (%TR), viability by the percentage of survived cells (%Survival), electric energy (W_e) was calculated as defined in Eq. 10 and the number of DNA molecules available for contact with the permeabilized surface (N_{DNA}) was obtained from Eqs. 7 and 8.

No interaction was observed when only a non-permeabilizing LV₃₀ pulse was applied. The detected TOTO fluorescence intensity FL^{TOTO} can be directly related to the N_{DNA} (Table 2), since the number of DNA molecules interacting with the permeabilized membrane is directly proportional to the plasmid concentration (Fig. 3). The HV+LV protocol yielded the highest FL^{TOTO} followed by the LV+HV and HV protocols for all c_{DNA} , in contrast to the %TR, where at optimal c_{DNA} the %TR was similar for all protocols. When we analyze the DNA-membrane interaction (FL^{TOTO}) in rela-

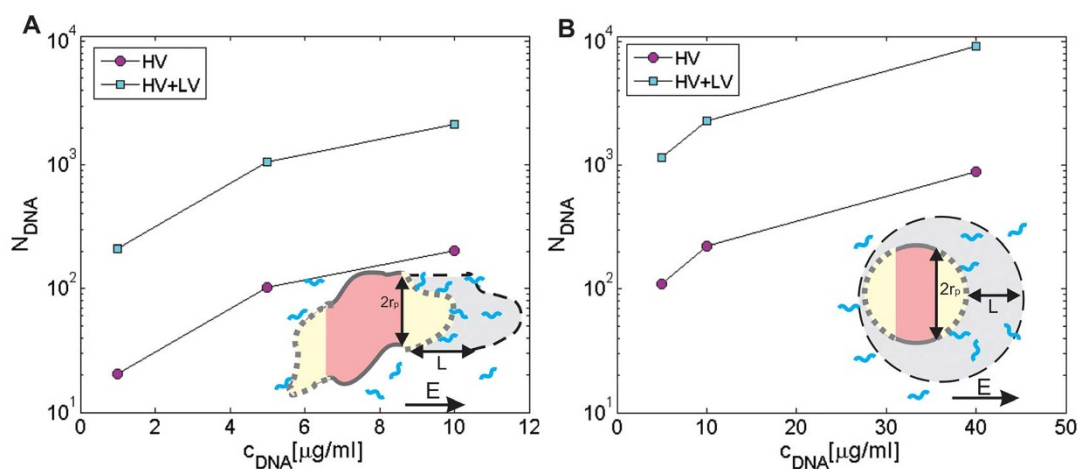


Figure 4 | Theoretical analysis of DNA accumulation at the cell membrane due to electrophoretic force. The number of DNA molecules (N_{DNA}) available for contact with the permeabilized part of the cell membrane for different plasmid c_{DNA} for plated cells (A) and cells in a suspension (B) are shown for HV and HV+LV pulses (corresponding transfection efficiencies are shown in Fig 1). The schematic representation shows the calculation of N_{DNA} , where L is the distance traveled due to electrophoresis and r_p is the radius of the permeabilized membrane (dotted, yellow area) for plated cells (A) and cells in a suspension (B). The gray shaded region represents the volume V from which DNA molecules are brought in contact with the cell membrane. The strength and length of pulses determine the distance L from which DNA can access the cell membrane (gray) and E determines the area of the membrane which is electroporated.



tion to the N_{DNA} we can see that there is a direct relation between the theoretically calculated number of DNA molecules and FL^{TOTO} , however, the DNA-membrane interaction is only one of several steps, and other factors such as DNA stability in the cytosol and cell viability are also crucial.

Another aspect is also how the fluorescence intensity of GFP (FL^{GFP}) is related to the N_{DNA} . Indeed, HV+LV pulses consistently resulted in a higher FL^{GFP} compared to HV pulses only, for both plated cells and cells in a suspension (Fig. 2) for all plasmid concentrations. This is also in agreement with other studies (6,14), where for relatively long pulses (8×5 ms) FL^{GFP} can be increased even if the maximal %TR is obtained. However, a statistically significant increase of FL^{GFP} for HV+LV pulses compared to HV was obtained only at the lowest c_{DNA} , while at the highest c_{DNA} the difference in FL^{GFP} between the two pulsing protocols was not statistically significant, which also suggests that at some point saturation is reached.

Discussion

Altogether our results confirm that electroporation is a crucial step for efficient gene delivery, in accordance with other reports^{10,30,34,35,36,59}. This was further confirmed by theoretical analyses of the %TR dependence on the fraction of permeabilized membrane surface S_e/S_0 , where approx. linear dependency was obtained⁴⁷. However, electrotransfection is a complex process and for cells in suspension the experimental values of %TR deviate from the linear curve (see Fig. 1B); thus, the assumption that S_e/S_0 directly correlates with %TR can only be a first approximation.

Further, electrophoresis of the pDNA in an electric field is also an important factor. In order to analyze electroporation and electrophoresis, we used different HV-LV pulsing protocols and different pDNA concentrations (c_{DNA}). We show that HV+LV pulsing protocols were more efficient in terms of percentage transfection (%TR) and fluorescence intensity (FL^{GFP}) compared to HV pulses only, especially for low c_{DNA} . For higher c_{DNA} , saturation in terms of maximal %TR was obtained while FL^{GFP} still increased for high c_{DNA} (see Fig. 2). For in vivo applications, it is important to also analyze the effect of the amplitude of the LV pulse on gene electrotransfer²⁴. We obtained that if LV is above the permeabilization threshold (e.g.

LV₅₅), a high %TR for HV+LV pulses can be attributed both to electrophoresis and to increased electroporation due to the LV pulse, while for sub-threshold low-voltage pulses (LV₃₀), LV has only an electrophoretic role.

We extended our previous studies on plated cells and cells in a suspension^{18,19,36} and analyzed the observed differences. This is relevant since cells in suspension are most often used in vitro, while plated cell are closer to in vivo conditions. A theoretical analysis is presented in Fig. 4, where the results of calculations of the N_{DNA} (the number of DNA molecules that are available for contact with the permeabilized cell membrane) for different pulsing protocols are shown.

Based on all the results of HV-LV pulses, we confirmed the hypothesis that in conditions where we reach saturation (high N_{DNA}), an additional electrophoretic LV pulse does not increase the %TR, while the GFP expression (FL^{GFP}) can still be increased (see Figs. 2 and 4). Theoretical analysis showed that the strength and length of the electric pulses determine the distance L from which DNA can access the cell, and E also determines the area (S_e) of the membrane which is electroporated. We could adequately explain the differences in transfection for different c_{DNA} , but some data still seemed puzzling. The observed differences in electrotransfection between plated cells and cells in a suspension can be explained by several specific characteristics of the attached cells and suspended cells. This is presented in Fig. 6, where a schematic representation of electroporation and electrotransfection of the plated cells (6A) and cells in a suspension (6B) is shown, and can be analyzed as follows:

- different forces acting on cells in a suspension during pulse delivery, like fluid flow and electrophoretic movement due to the cells' negative surface charge, lead to the displacement and rotation of the cells. This leads to permeabilization of a larger area of the cell membrane (see Fig. 6B), which makes more binding sites available for DNA and increases the maximal N_{DNA} as shown in Fig. 4B, thus allowing more DNA molecules to be transferred. It was shown previously³⁰ that cell electroporation and electrotransfer form different sides, enables higher transfection efficiency. Thus, the rotation of

Table 2 | Quantification of the process related to the different steps of gene electrotransfer: electroporation – PI uptake (%PI), DNA-membrane interaction represented by the fluorescence intensity of TOTO-labeled DNA (FL^{TOTO}), gene expression represented by the fluorescence intensity of GFP (FL^{GFP}), percentage of transfection (%TR), viability (%survival) for $c_{DNA} = 10 \mu\text{g/ml}$, electric energy obtained from Eq. 10 (W_e), and estimation of DNA accumulation at the cell membrane – the calculation of number of DNA molecules (N_{DNA}) interacting with the permeabilized cell membrane calculated from Eqs. 7 and 8 for different pulsing protocols: HV: $4 \times 200 \mu\text{s}$, 1.0 kV/cm, 1 Hz; LV: $1 \times 100 \text{ms}$, 0.075 kV/cm*. All data are given for plated CHO cells; for better readability only mean values are given

Pulsing protocol	Permeabilisation	Interaction	Transfection		Viability	El. energy	Electro-phoresis
	%PI	$^aFL^{TOTO}$ [A.U.]	FL^{GFP} [A.U.]	%TR	%Survival	$W_e/k = E^2 \times t_e \text{ms} \times (\text{kV/cm})^2$	N_{DNA}
HV							
$c_{DNA} = 1 \mu\text{g/ml}$	82.9%	343	658	6%	82%	0.8	20
$c_{DNA} = 10 \mu\text{g/ml}$		1073	2004	25%			200
HV+LV							
$c_{DNA} = 1 \mu\text{g/ml}$	85.9%	772	1769	23%	91%	1.36	250
$c_{DNA} = 10 \mu\text{g/ml}$		3469	2852	27%			2500
LV+HV							
$c_{DNA} = 1 \mu\text{g/ml}$	85.9% ^b	527	904	13%	87%	1.36	20–250
$c_{DNA} = 10 \mu\text{g/ml}$		1386	1819	21%			200–2500 ^b
LV							
$c_{DNA} = 1 \mu\text{g/ml}$	1.5%	187	208	0.9%	78%	0.56	0 ^d
$c_{DNA} = 10 \mu\text{g/ml}$		289 ^c	258	0.3%			

^afor observation of DNA-membrane interaction, we used 2 $\mu\text{g/ml}$ DNA and 1.4 kV/cm short-duration pulses instead of 1.0 kV/cm (see the M&M section) and for LV, 0.137 kV/cm instead of 0.075 kV/cm.

^bsince LV is applied before HV, it contributes only to accumulation but not to insertion; the %PI is taken from the HV+LV protocol.

^csimilar to the background value.

^dthe permeabilized surface is zero (see Theoretical section).

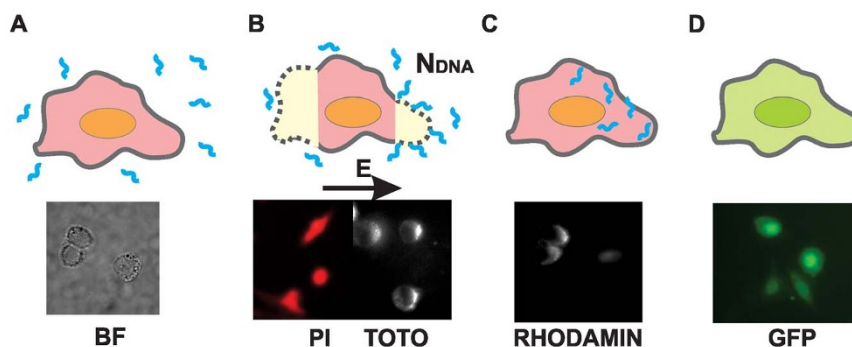


Figure 5 | Different steps of gene electrotransfer. (A) DNA is added to the electropermeabilization buffer, (B) electropermeabilization of the cell membrane and DNA contact/insertion with/into the membrane, (C) transfer across the membrane and into the nucleus, (D) gene expression. Corresponding fluorescence images below: electropermeabilization (PI), interaction of DNA with the membrane (TOTO), transfer into cytoplasm (RHODAMIN) and gene expression (GFP).

- suspended cells enables higher transfection (Fig. 6). In addition, for plated cells due to geometry (cells are spread on the surface) smaller surface is available for DNA binding/insertion. This explains why saturation is reached at much higher N_{DNA} values for cells in a suspension compared to plated cells (see Figs. 2 and 4). It also explains partially why the overall maximal %TR can be much higher in a suspension;
- ii) with a very low c_{DNA} in a suspension, there is a very low probability of N_{DNA} insertion into the membrane, since there is only a small number of molecules available for contact, and in combination with the movement of cells (displacement and rotation) in a suspension (Fig. 6B), this leads to a very low overall transfection for lower plasmid concentrations. Therefore, the c_{DNA} for suspensions has to be increased compared to plated cells, where cells are attached to the surface and all DNA in the vicinity can form a contact with the membrane. For increasing c_{DNA} and higher N_{DNA} , the transfection efficiency can be significantly increased in a suspension, and saturation is only reached at very high numbers of N_{DNA} ($\sim 10^3$), as shown in Fig. 4B. In contrast, with plated cells saturation is already reached at much smaller c_{DNA} and N_{DNA} (~ 300), as can be seen in Fig. 4A, since the entire permeabilized surface is already occupied by DNA molecules.
 - iii) the overall maximal %TR in a suspension is much higher than in plated cells (Fig. 1), but this is logical if we take into account that cells in a suspension have a very homogenous distribution of sizes. Thus, with optimal pulses most of the cells are permeabilized and remain viable, enabling good electrotransfer efficiency. On the other hand, plated cells are of different sizes and non-spherical shapes, with large variations in the minimal

and maximal diameter, and with different orientations (Fig. 6A)^{36,57}. Therefore, optimal pulses for the transfection of some cells directly lead to the irreversible electropermeabilization or poor transfection of other cells. Thus, saturation for high N_{DNA} and maximal %TR is limited for plated cells, due also to the non-homogeneous distribution of sizes and shapes.

Further, we can assume two hypothesis regarding the most important parameters relevant for efficient electrotransfer; i) the electric energy of the pulses is the crucial parameter for efficient transfection or ii) the number of DNA molecules available for contact with the permeabilized membrane (N_{DNA}) is the most relevant parameter. Based on the presented data and theoretical analysis, we can assume that not W_e but the accumulation of DNA molecules at the permeabilized membrane surface (N_{DNA}) is the most important factor. N_{DNA} is approximately linearly dependent on the E , t_E , c_{DNA} and permeabilized membrane surface S_c :

$$N_{DNA} \propto c_{DNA} E t_E (1 - (E_c/E)^2). \quad (11)$$

The assumption that the electrotransfer efficiency is proportional to N_{DNA} is only an approximation, since these are stochastic processes and consequently the probability of electrotransfer is proportional to the N_{DNA} available for electrotransfer until saturation is reached (explained below). From Table 2, it is clear that W_e could not be the only factor for efficient gene transfer, since the energy of the LV pulse alone is of the same order of magnitude as the energy of HV pulses, while transfection is negligible for the LV pulse. Electric energy also cannot explain the results obtained for the different c_{DNA} .

On the other hand, N_{DNA} is the parameter that is directly related with experimental results, especially for sub-optimal pDNA concen-

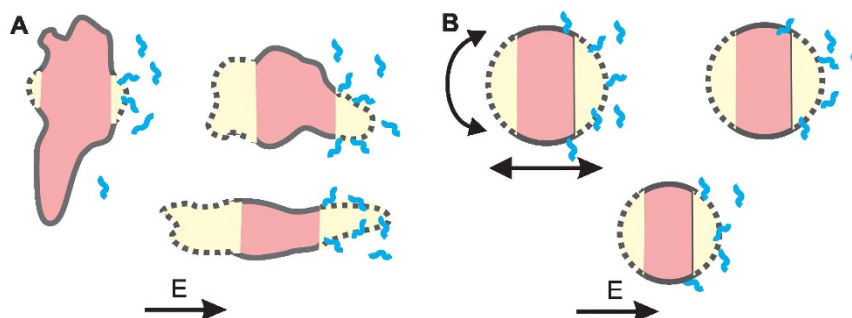


Figure 6 | Schematic representation of electrotransfection of plated cells (A) and cells in a suspension (B). Cells in a suspension are spherical and with a narrow distribution of sizes, while plated cells have large variations in size, orientation and shape. Consequently, for plated cells it is very difficult to achieve pulses that would enable optimal electropermeabilization (yellow) and electrotransfer of all cells, in contrast to cells in suspension where this is possible. Furthermore, cells in a suspension rotate and move during pulses, thus a higher N_{DNA} is needed and therefore a higher c_{DNA} must be used compared to plated cells.



trations. It can be seen that the N_{DNA} for HV+LV pulses (250) for the lowest pDNA concentration (1 $\mu\text{g/ml}$) on plated cells is similar to the N_{DNA} for HV pulses only (200) at the highest $c_{DNA} = 10 \mu\text{g/ml}$, which is in agreement with similar values of %TR (23% and 25%) obtained experimentally (Table 2). Therefore, %TR is directly related to N_{DNA} up to the point where saturation is reached, and an increase in N_{DNA} does not lead to a higher %TR (for plated cells saturation is reached at $N_{DNA} \cong 250$). Consequently, we can explain why at $c_{DNA} = 10 \mu\text{g/ml}$, the HV+LV pulsing protocol ($N_{DNA} \cong 2500$) was similarly effective as the HV protocol ($N_{DNA} \cong 250$) for plated cells (approx. 25% TR for both protocols). For the LV+HV protocol, this is not so clear since LV is applied before permeabilizing HV pulses, and thus it contributes only to the accumulation but not to the insertion of pDNA into the membrane.

Therefore, the second hypothesis – that the number of DNA molecules interacting with the permeabilized cell membrane is a more relevant parameter – seems more plausible. If we analyze N_{DNA} , it can be seen that electroporation is important for low c_{DNA} , where the accumulation of DNA at the membrane is a limiting factor (Table 2), while for higher c_{DNA} the saturation is reached. Therefore, the %TR is directly related to N_{DNA} for sub-optimal plasmid concentrations, while for higher c_{DNA} the %TR does not depend directly on N_{DNA} due to saturation.

If we now summarize the main results in Table 2, we can see that there is a direct relation between the DNA-membrane interaction FL^{TOTO} with the transfection efficiency (FL^{GFP} and %TR) for lower plasmid concentrations. For increased c_{DNA} (10 $\mu\text{g/ml}$), saturation is reached in terms of maximal %TR and partially for FL^{GFP} . Therefore, at some point even if N_{DNA} interacting with the membrane FL^{TOTO} is increased, the %TR cannot be increased. This clearly shows on one hand that the transfection efficiency is directly related to electroporation, and that it is a stochastic process in which more DNA in contact with the permeabilized part of the membrane enables more molecules to enter. But at some point, there is saturation as the process becomes similar to a chemical process, where there is a limited number of binding sites, naturally leading to saturation.

Another important aspect is also the physiological state of the cell and its viability, which limits transfection efficiency; namely the total yield of transfected cells is lowered since some cells are very effectively transfected while others are in poor physiological condition or die due to extensive membrane damage and the loss of cell homeostasis. Thus, depending on the type of application, the selection of the specific pulsing protocol depends on whether high yield or high loading is needed. Thus, we proposed²¹ that in *in vitro* conditions for a high number of copies transferred, it is advisable to use long-duration millisecond pulsing protocols or a combination of HV+LV pulses^{10,35,43}, while for certain biomedical and biotechnological applications where the total yield of transfected cells and/or preserved viability is crucial (e.g. immuno-gene therapy)⁹, short-duration pulse protocols are more optimal. We have to stress, however, that *in vivo* the differences between tissue properties also determine the choice of optimal electric pulse parameters.

Further, we addressed another open question: how does DNA cross the cell membrane and enter the cytosol? There are two main hypotheses of DNA entry, as schematically presented in Fig. 7 above. The first hypothesis suggests that DNA is first inserted into the permeabilized cell membrane and is then transferred into the cytosol by some unknown mechanism^{15,16,19,60} (Fig. 7A). Alternatively, the second hypothesis assumes that DNA-membrane complex formation, in combination with exposure to an electric field, triggers endocytotic invagination of the cell membrane (Fig. 7B), followed by the transfer of DNA into the cytosol. However, endocytotic entry has thus far been directly confirmed only in a few reports^{32,46}. No direct observation of DNA transfer across the membrane has been observed; direct visualization only showed^{21,29,30} that formation of a stable DNA-membrane complex occurs on a time scale of 1 s after EP

and that DNA enters in minutes after pulse application^{29,30}. Our results confirmed that DNA enters the cytosol in minutes after pulse delivery as shown in Fig. 5C. However, when we designed a separated study to analyze the role of electrostimulated endocytosis in gene electrotransfer, we have not confirmed this hypothesis⁴⁷ for our pulsing protocol. Visualization of endocytotic vesicles after the application of our HV pulses showed that the level of endocytosis did not increase above the threshold electric field for electrotransfer, suggesting that electro-endocytosis is not the dominant mechanism for electrotransfer with this protocol. Also in studies^{21,29,30} where TOTO-labeled pDNA was used for analysis of the interaction with the membrane, no endocytotic uptake was observed – in our experiments fluorescence spots were also observed 15 min after electroporation, only on the cell membrane (results not shown) and not in the cytoplasm.

Further, by using HV+LV and the reversed order of LV+HV pulses, we could indirectly analyze the mechanism of how DNA enters the cytosol. However, since a significantly higher transfection efficiency and DNA-membrane interaction was observed for HV+LV compared to the LV+HV protocol (Table 2) at sub-optimal 1 $\mu\text{g/ml}$ c_{DNA} , we propose that the LV pulse applied after HV pulses is crucial for DNA insertion and/or translocation across the cell membrane, and not only for accumulation of DNA at the cell membrane surface. This further supports the hypothesis that DNA is first inserted into the permeabilized membrane and later enters the cytoplasm via translocation across the membrane pores (Fig. 7A).

Taking into account all results of our and other studies, we propose that DNA insertion into the permeabilized membrane during electric pulses is a first and crucial step for later DNA entry via either translocation or electroendocytosis (Fig. 7B), and that the way of DNA entry might also depend on the specific pulsing protocol. The process probably involves DNA interaction with the permeabilized cell membrane and not only the simple contact of the DNA with the membrane. The possible mechanism of DNA translocation through electropores could be a mechanism similar to the Brownian ratchet, which was described for nucleotide translocation through nanopores due to entropic forces^{19,61,62}. So far the most developed theoretical description of electroporation is a model of formation of aqueous pores in the membrane², and a very consistent and experimentally verified theoretical framework was also presented describing pore formation and resealing⁶³. However, for electrotransfection no such theoretical description exists, thus the mechanism of DNA entry is still an open question.

The last step for successful electrotransfer is the entry of pDNA into the nucleus, since the nuclear envelope is not permeabilized by the standard electroporation pulses commonly used. The majority of plasmids including pDNA, used in our study have the NLS sequence for enhanced transport into the nucleus encoded in SV 40 DLS^{31,52}. In spite of the NLS sequence, better electrotransfer efficiency is obtained in mitotic cells^{49,51}, confirmed also in our experiments. We obtained an approx. 3 \times times higher %TR for cells in an exponential phase compared to cells in a plateau phase (arrested in the G1 phase), as shown in Table 1. This is especially important for clinical applications since most of the somatic cells in tissues are not actively dividing. It was shown that plasmid containing a specific NLS designed for a particular target tissue can significantly improve the transfer efficiency⁵³.

Conclusions

In this paper we integrate an experimental and theoretical analysis of the different steps involved in gene electrotransfer in order to gain new insights into the processes involved. We show that the number of DNA molecules in contact with a permeabilized membrane is governed by the electroporation surface, the electrophoretic force and the pDNA concentration. The inserted DNA is slowly transferred into the cytosol in minutes following the pulses.

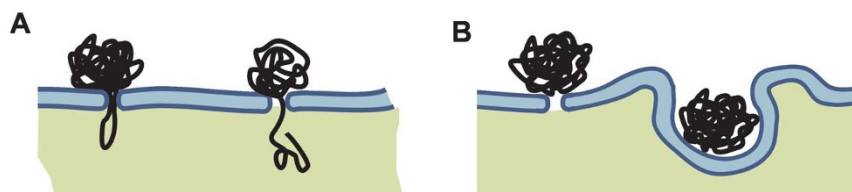


Figure 7 | Two possible hypotheses of DNA entry into the cytoplasm. (A) DNA is inserted into the permeabilized cell membrane during electric pulses and is translocated inside the cell by a slow process after pulse delivery; (B) DNA interacts with the permeabilized membrane and is consequently endocytosed.

Nuclear entry can be a limiting factor for *in vivo* application where cells are not actively dividing, while *in vitro* cells in the exponential growth phase must be used for optimal transfection. We also explain the differences between the electrotransfer efficiency of suspended and plated cells; the later represent a more relevant system for *in vivo* applications, while cell suspensions enable a higher transfection yield due to the more homogeneous size, shape and movement of suspended cells.

For different HV-LV pulsing protocols, we analyzed the crucial parameters: from DNA interaction with the permeabilized cell membrane (N_{DNA}) to the observed transfection efficiency (%TR, FL^{GFP}), and their mutual relations. We obtained that N_{DNA} and FL^{TOTO} increase with higher DNA concentrations or with the addition of LV pulses, while %TR and FL^{GFP} both reach saturation. Therefore, direct correlation between interaction and transfection efficiency exists only to a certain point where saturation is reached, due to a limited number of DNA molecules that can interact with the permeabilized surface of the membrane and consequently be transferred.

By understanding the interplay of these parameters, one can design a more optimal electric protocol for a specific application, where either high loading of the plasmid with moderate cell viability or moderate transfection efficiency with preserved viability can be obtained. Further, pDNA concentration is also important: for sub-optimal c_{DNA} (realistic for *in vivo* conditions), saturation is not reached, thus electrophoresis plays an important role, while for optimal c_{DNA} (high N_{DNA}) a higher transfection yield can be achieved (e.g. *in vitro*). Finally, as a mechanism of DNA electrotransfer into cells, we propose that after insertion into the permeabilized membrane, DNA is either translocated into the cytoplasm after the pulses by some relatively slow mechanism such as Brownian ratchet, or alternatively it may be transferred by electric-field stimulated endocytosis, or both, where the mechanism probably depends on the choice of pulse parameters.

1. Neumann, E., Schaefferidder, M., Wang, Y. & Hofschneider, P. Gene-transfer into mouse lyoma cells by electroporation in high electric-fields. *EMBO J.* **1**, 841–845 (1982).
2. Weaver, J. C. & Chizmadzhev, Y. A. Theory of electroporation: A review. *Bioelectrochem. Bioenerg.* **41**, 135–160 (1996).
3. Titomirov, A., Sukharev, S. & Kistanova, E. *In vivo* electroporation and stable transformation of skin cells of newborn mice by plasmid DNA. *Biochim. Biophys. Acta* **1088**, 131–134 (1998).
4. Heller, R. *et al.* *In vivo* gene electroinjection and expression in rat liver. *FEBS Lett.* **389**, 225–228 (1996).
5. Aihara, H. & Miyazaki, J. Gene transfer into muscle by electroporation *in vivo*. *Nat. Biotechnol.* **16**, 867–870 (1998).
6. Rols, M. P., Delteil, C., Golzio, M. & Teissie, J. *In vitro* and *ex vivo* electrically mediated permeabilization and gene transfer in murine melanoma. *Bioelectrochem. Bioenerg.* **47**, 129–134 (1998).
7. Suzuki, T., Shin, B. C., Fujikura, K., Matsuzaki, T. & Takata, K. Direct gene transfer into rat liver cells by *in vivo* electroporation. *FEBS Lett* **425**, 436–440 (1998).
8. Mir, L. M., Bureau, M. F., Rangara, R., Schwartz, B. T. & Scherman, D. Long-term, high level *in vivo* gene expression after electric pulse-mediated gene transfer into skeletal muscle. *Comptes Rendus Acad. Sci. Ser. Iii-Sci. Vie-Life Sci.* **321**, 893–899 (1998).
9. Heller, R., Lundberg, C., Li, F., Burcus, N. & Shirley, S. Effective gene electrotransfer is dependent on the pulse parameters of the applied electric field. *Mol. Ther.* **21**, S41–S41 (2013).

10. Hojman, P. Basic principles and clinical advancements of muscle electrotransfer. *Curr. Gene Ther.* **10**, 128–138 (2010).
11. Daud, A. I. *et al.* Phase I trial of interleukin-12 plasmid electroporation in patients with metastatic melanoma. *J. Clin. Oncol.* **26**, 5896–5903 (2008).
12. Čemazar, M. *et al.* Control by pulse parameters of DNA electrotransfer into solid tumors in mice. *Gene Ther.* **16**, 635–644 (2009).
13. Ferber, D. Gene therapy: Safer and virus-free? *Science* **294**, 1638–1642 (2001).
14. Rols, M.-P. & Teissie, J. Electroporation of mammalian cells to macromolecules: control by pulse duration. *Biophys. J.* **75**, 1415–1423 (1998).
15. Klenchin, V., Sukharev, S., Serov, S., Chernomordik, L. & Chizmadzhev, Y. Electrically induced DNA uptake by cells is a fast process involving DNA electrophoresis. *Biophys. J.* **60**, 804–811 (1991).
16. Sukharev, S., Klenchin, V., Serov, S., Chernomordik, L. & Chizmadzhev, Y. Electroporation and electrophoretic DNA transfer into cells - the effect of DNA interaction with electropores. *Biophys. J.* **63**, 1320–1327 (1992).
17. Satkauskas, S. *et al.* Electrophoretic component of electric pulses determines the efficacy of *in vivo* DNA electrotransfer. *Hum. Gene Ther.* **16**, 1194–1201 (2005).
18. Kanduđer, M., Miklavčič, D. & Pavlin, M. Mechanisms involved in gene electrotransfer using high- and low-voltage pulses — An *in vitro* study. *Bioelectrochem.* **74**, 265–271 (2009).
19. Pavlin, M., Flisar, K. & Kanduđer, M. The role of electrophoresis in gene electrotransfer. *J. Membr. Biol.* **236**, 75–79 (2010).
20. Kanduđer, M. & Pavlin, M. [Gene electrotransfer: From understanding the mechanisms to optimization of parameters in tissues] *Advances in Planar Lipid Bilayers and Liposomes* [Iglič, A. (ed.)] [77–104] (Elsevier, Amsterdam, 2012).
21. Haberl, S. *et al.* Effect of different parameters used for *in vitro* gene electrotransfer on gene expression efficiency, cell viability and visualization of plasmid DNA at the membrane level. *J. Gene Med.* **15**, 169–181 (2013).
22. Zupanič, A., Čorović, S., Miklavčič, D. & Pavlin, M. Numerical optimization of gene electrotransfer into muscle tissue. *Biomed. Eng. Online* **9**, 66 (2010).
23. Prud'homme, G. J., Glinka, Y., Khan, A. S. & Draghia-Akli, R. Electroporation-enhanced nonviral gene transfer for the prevention or treatment of immunological, endocrine and neoplastic diseases. *Curr. Gene Ther.* **6**, 243–273 (2006).
24. Sallberg, M., Frelin, L. & Weiland, O. DNA vaccine therapy for chronic hepatitis C virus (HCV) infection: immune control of a moving target. *Expert Opin. Biol. Ther.* **9**, 805–815 (2009).
25. Low, L. *et al.* DNA Vaccination with electroporation induces increased antibody responses in patients with prostate cancer. *Hum. Gene Ther.* **20**, 1269–1278 (2009).
26. Van Druenen Littel-van den Hurk, S. & Hannaman, D. Electroporation for DNA immunization: clinical application. *Expert Rev. Vaccines* **9**, 503–517 (2010).
27. Golzio, M. *et al.* Observations of the mechanisms of electromediated DNA uptake from vesicles to tissues. *Curr. Gene Ther.* **10**, 256–266 (2010).
28. Andre, F. M. & Mir, L. M. Nucleic acids electrotransfer *in vivo*: mechanisms and practical aspects. *Curr. Gene Ther.* **10**, 267–280 (2010).
29. Golzio, M., Teissie, J. & Rols, M.-P. Direct visualization at the single-cell level of electrically mediated gene delivery. *Proc. Natl. Acad. Sci.* **99**, 1292–1297 (2002).
30. Faurie, C. *et al.* Electro-mediated gene transfer and expression are controlled by the life-time of DNA/membrane complex formation. *J. Gene Med.* **12**, 117–125 (2010).
31. Vaughan, E. & Dean, D. Intracellular trafficking of plasmids during transfection is mediated by microtubules. *Mol. Ther.* **13**, 422–428 (2006).
32. Rosazza, C. *et al.* Cholesterol implications in plasmid DNA electrotransfer: Evidence for the involvement of endocytotic pathways. *Int. J. Pharm.* **423**, 134–143 (2012).
33. Kinoshita, K. & Tsong, T. Voltage-Induced Conductance in Human-Erythrocyte Membranes. *Biochim. Biophys. Acta.* **554**, 479–497 (1979).
34. Wolf, H., Rols, M.-P., Boldt, E., Neumann, E. & Teissie, J. Control by pulse parameters of electric field-mediated gene-transfer in mammalian cells. *Biophys. J.* **66**, 524–531 (1994).
35. Gehl, J. *et al.* *In vivo* electroporation of skeletal muscle: threshold, efficacy and relation to electric field distribution. *Biochim. Biophys. Acta-Gen. Subj.* **1428**, 233–240 (1999).
36. Marjanović, I., Haberl, S., Miklavčič, D., Kanduđer, M. & Pavlin, M. Analysis and comparison of electrical pulse parameters for gene electrotransfer of two different cell lines. *J. Membr. Biol.* **236**, 97–105 (2010).



37. Neumann, E., Kakorin, S., Tsoneva, I., Nikolova, B. & Tomov, T. Calcium-mediated DNA adsorption to yeast cells and kinetics of cell transformation by electroporation. *Biophys. J.* **71**, 868–877 (1996).
38. Xie, T. & Tsong, T. Study of mechanisms of electric-field-induced DNA transfection 5. Effects of DNA topology on surface binding, cell uptake, expression, and integration into host chromosomes of DNA in the mammalian cell. *Biophys. J.* **65**, 1684–1689 (1993).
39. Haberl, S., Miklavčič, D. & Pavlin, M. Effect of Mg ions on efficiency of gene electrotransfer and on cell electropermeabilization. *Bioelectrochem.* **79**, 265–271 (2010).
40. Zaharoff, D. A., Barr, R. C., Li, C. Y. & Yuan, F. Electromobility of plasmid DNA in tumor tissues during electric field-mediated gene delivery. *Gene Ther.* **9**, 1286–1290 (2002).
41. Zaharoff, D. A. & Yuan, F. Effects of pulse strength and pulse duration on in vitro DNA electromobility. *Bioelectrochem.* **62**, 37–45 (2004).
42. Haberl, S. & Pavlin, M. Use of collagen gel as a three-dimensional in vitro model to study electropermeabilization and gene electrotransfer. *J. Membr. Biol.* **236**, 87–95 (2010).
43. André, F. M. *et al.* Efficiency of high- and low-voltage pulse combinations for gene electrotransfer in muscle, liver, tumor, and skin. *Hum. Gene Ther.* **19**, 1261–1272 (2008).
44. Xie, T., Sun, L. & Tsong, T. Study of mechanisms of electric field-induced DNA transfection. 1. DNA entry by surface binding and diffusion through membrane pores. *Biophys. J.* **58**, 13–19 (1990).
45. Zimmermann, U. *et al.* Mechanisms of Electrostimulated Uptake of Macromolecules into Living Cells. *Naturwissenschaften* **77**, 543–545 (1990).
46. Wu, M. & Yuan, F. Membrane binding of plasmid DNA and endocytic pathways are involved in electrotransfection of mammalian cells. *PLoS ONE* **6**, e20923 (2011).
47. Pavlin, M., Pucihar, G. & Kandušer, M. The role of electrically stimulated endocytosis in gene electrotransfer. *Bioelectrochem.* **83**, 38–45 (2012).
48. Lechardeur, D., Verkman, A. & Lukacs, G. Intracellular routing of plasmid DNA during non-viral gene transfer. *Adv. Drug Deliv. Rev.* **57**, 755–767 (2005).
49. Yorifuji, T., Tsuruta, S. & Mikawa, H. The effect of cell synchronization on the efficiency of stable gene-transfer by electroporation. *FEBS Lett.* **245**, 201–203 (1989).
50. Miller, A. M. & Dean, D. A. Cell-specific nuclear import of plasmid DNA in smooth muscle requires tissue-specific transcription factors and DNA sequences. *Gene Ther.* **15**, 1107–1115 (2008).
51. Golzio, M., Teissié, J. & Rols, M.-P. Cell synchronization effect on mammalian cell permeabilization and gene delivery by electric field. *Biochim. Biophys. Acta BBA-Biomembr.* **1563**, 23–28 (2002).
52. Lam, A. P. & Dean, D. A. Progress and prospects: nuclear import of nonviral vectors. *Gene Ther.* **17**, 439–447 (2010).
53. Young, J. L., Zimmer, W. E. & Dean, D. A. Smooth muscle-specific gene delivery in the vasculature based on restriction of DNA nuclear import. *Exp. Biol. Med.* **233**, 840–848 (2008).
54. Maucksch, C. *et al.* Transgene expression of transfected supercoiled plasmid DNA concatemers in mammalian cells. *J. Gene Med.* **11**, 444–453 (2009).
55. Henshaw, J. W., Zaharoff, D. A., Mossop, B. J. & Yuan, F. Electric field-mediated transport of plasmid DNA in tumor interstitium in vivo. *Bioelectrochem.* **71**, 233–242 (2007).
56. Schwan, H. P. & Pauly, H. Impedance of a suspension of ball-shaped particles with a shell; a model for the dielectric behavior of cell suspensions and protein solutions. *Z Naturforsch B.* **14B**, 125–31 (1959).
57. Valič, B. *et al.* Effect of electric field induced transmembrane potential on spheroidal cells: theory and experiment. *Eur. Biophys. J.* **32**, 519–528 (2003).
58. Schwister, K. & Deuticke, B. Formation and properties of aqueous leaks induced in human-erythrocytes by electrical breakdown. *Biochim. Biophys. Acta.* **816**, 332–348 (1985).
59. Bureau, M. F. *et al.* Muscle transfection and permeabilization induced by electrotransfer or pluronic® L64. Paired study by optical imaging and MRI. *Biochim. Biophys. Acta BBA - Gen. Subj.* **1800**, 537–543 (2010).
60. Bureau, M. F., Gehl, J., Deleuze, V., Mir, L. M. & Scherman, D. Importance of association between permeabilization and electrophoretic forces for intramuscular DNA electrotransfer. *Biochim. Biophys. Acta-Gen. Subj.* **1474**, 353–359 (2000).
61. De Gennes, P.-G. Passive entry of a DNA molecule into a small pore. *Proc. Natl. Acad. Sci.* **96**, 7262–7264 (1999).
62. Kasianowicz, J. J., Brandin, E., Branton, D. & Deamer, D. W. Characterization of individual polynucleotide molecules using a membrane channel. *Proc. Natl. Acad. Sci.* **93**, 13770–13773 (1996).
63. Saulis, G. Pore disappearance in a cell after electroporation: Theoretical simulation and comparison with experiments. *Biophys. J.* **73**, 1299–1309 (1997).

Acknowledgments

The authors would like to thank Karel Flisar, who developed the pulse generator prototype, which enabled us to switch the time-course of HV and LV pulses, and also Matej Reberšek and Vilko Leben, who were involved in the development of several new high-voltage generators. We also thank Mateja Manček Keber from the National Chemistry Institute in Ljubljana for help with flow cytometry. We also thank our graduated and PhD students Igor Marjanovič, Maruša Stražišar and Saša Haberl, who performed some parts of the experiments and to Duša Hodžič, for preparation of pDNA. We would also like to thank Muriel Golzio and Marie Pierre Rols from CNRS Toulouse, France, for their useful suggestions with the TOTO protocol. M.K. would also like to thank Damijan Miklavčič, head of Laboratory of Biocybernetics, for his general support. This work was supported by the Slovenian Research Agency within projects J2-9770, J4-4324, P2-0249, J3-6794 and the MRIC UL IP-0510 Infrastructure Program.

Author contributions

M.P. and M.K. wrote the manuscript text, prepared all figures, and designed and performed the experiments. M.P. performed the theoretical calculations and analysis. Both M.P. and M.K. reviewed and approved the manuscript.

Additional information

Competing financial interests: The authors declare no competing financial interests.

How to cite this article: Pavlin, M. & Kandušer, M. New Insights into the Mechanisms of Gene Electrotransfer – Experimental and Theoretical Analysis. *Sci. Rep.* **5**, 9132; DOI:10.1038/srep09132 (2015).



This work is licensed under a Creative Commons Attribution 4.0 International License. The images or other third party material in this article are included in the article's Creative Commons license, unless indicated otherwise in the credit line; if the material is not included under the Creative Commons license, users will need to obtain permission from the license holder in order to reproduce the material. To view a copy of this license, visit <http://creativecommons.org/licenses/by/4.0/>